
Trained Persistent Memory for Frozen Encoder–Decoder LLMs: Six Architectural Methods

Hong Jeong

Inha University in Tashkent, Uzbekistan
hjeong@postech.ac.kr

Abstract

Frozen encoder–decoder language models are stateless: the latent representation is discarded after every forward pass, so no information persists across sessions. This paper presents a **proof-of-concept pilot study** showing that persistent memory in the *continuous latent space* of a frozen LLM is feasible—even under severe resource constraints (a single frozen Flan-T5-XL backbone, small trainable adapters, a single dataset). We implement six architectural methods spanning three injection points and four write mechanisms; unlike text-level memory systems, every write and read is a differentiable operation on dense vectors. After training only the adapter, the memory bank continues to accumulate at inference time without gradients, enabling *conversational learning*. Under a forgetting-curve evaluation on LoCoMo at two capacity scales ($1\times$ and $10\times$), the stateless baseline scores exactly zero; at $10\times$ all six trained adapters produce positive memory-recall curves; at $1\times$ three methods collapse, revealing capacity as a critical design parameter. Because the memory bank is a compact numerical array, it can be scaled to arbitrarily large capacity without altering the backbone. We argue that full end-to-end training with larger models, larger data, and orders-of-magnitude larger memory will yield substantially stronger results; this pilot study establishes the feasibility baseline and design-space taxonomy that such efforts require.

1 Introduction

Consider a frozen encoder–decoder model such as Flan-T5 built on a T5-style backbone [1]. The forward pass is:

$$Z_t = E_{\text{frozen}}(x_t), \quad \hat{y}_t = D_{\text{frozen}}(Z_t), \quad (1)$$

where E_{frozen} and D_{frozen} are fixed pre-trained weights, x_t is the input at turn t , $Z_t \in \mathbb{R}^{n \times d}$ is the encoder output, and \hat{y}_t is the generated text. This system is **stateless**: Z_t is discarded after each forward pass and the model has no recollection of previous turns. If a user says “I like reading” in session 1 and asks “What do I like?” in session 3, the model cannot answer—there is no state that survives across sessions. This *inter-session memory* problem is the concrete target of persistent memory.

Existing long-term memory solutions such as MemGPT and MemoryBank operate at the *text level*: they store, summarize, and retrieve natural-language passages through an external database. This paper works at a fundamentally different level—the **latent space** of the frozen model. The memory bank $P_t \in \mathbb{R}^{n_P \times d}$ holds continuous encoder representations, not strings, so writing and reading are differentiable operations embedded inside the forward pass rather than pre- or post-processing steps around it.

A persistent bank built directly from frozen encoder outputs is not enough. The decoder’s cross-attention was pre-trained to read current encoder states, not arbitrarily accumulated cache states, so a naive memory path tends to dilute attention rather than sharpen retrieval as history grows. Recent attention-coupled latent-memory work shows that learned structure inside the memory pathway can instead induce functional specialization and controlled routing [6, 7]. For frozen encoder–decoder LLMs, this suggests that a small trainable adapter is the minimal mechanism needed to write memory in a form the frozen decoder can use.

This paper takes the necessary next step: we **allow training** for a small memory adapter θ_{Mem} while keeping both encoder and decoder frozen. We augment the stateless system with a **persistent memory bank** $P_t \in \mathbb{R}^{n_P \times d}$ that persists across turns and sessions:

$$Z_t = E_{\text{frozen}}(x_t), \quad P_t = \text{Write}(P_{t-1}, Z_t), \quad \hat{y}_t = D_{\text{frozen}}(\text{Read}(Z_t, P_{t-1})). \quad (2)$$

The `Write` operation updates P from the current latent; the `Read` operation injects historical context from P into the decoder. The learned parameters θ_{Mem} enable the adapter to *learn how to write memory in a format that the frozen decoder’s existing cross-attention can discriminate*—the capability that zero-training methods provably lack.

This paper is deliberately designed as a **low-budget pilot study**: we use a single frozen backbone, a single evaluation dataset, and minimal adapter parameters. The goal is not to achieve state-of-the-art recall but to *demonstrate feasibility*—that persistent latent-space memory can be installed in an existing frozen LLM with inexpensive adapters, and that the resulting system exhibits non-trivial, capacity-dependent memory behaviour. Full end-to-end training with unfrozen, larger-scale LLMs, bigger datasets, and memory banks orders of magnitude larger than ours lies beyond the scope of this pilot but is the natural industrial-scale follow-up that our results motivate.

Empirically, even under these constrained conditions the six designs separate clearly. At $10\times$ capacity all trained adapters rise above the zero baseline on the forgetting curve; at $1\times$ three methods collapse. M.2 XAttn and M.6 Slot dominate at low capacity, while M.4 Hebbian leads at high capacity—revealing memory-bank size as a critical design parameter.

After training, θ_{Mem} is frozen but P_t continues to accumulate at inference time without gradients. We call this **conversational learning**: each new session enriches P , so a fact stated in session 1 (“I am John Doe”) can be recalled in session 10 (“Who am I?”) without re-stating it and without million-token context windows—the relevant inter-session history is compressed into P .

The analogy to human cognition is deliberate. Human brains accumulate knowledge through complementary memory systems [8]: *episodic* memory records specific events (“Alice mentioned a trip to Paris”), *semantic* memory distills general facts (“Alice likes travel”), *procedural* memory encodes how-to skills, and *working memory* holds the active conversational context. All of these are linked through *associative* retrieval: a cue in working memory can trigger recall from any long-term store. The persistent memory bank P in our framework plays an analogous role: the write rule determines what is stored (episodic vs. semantic), the read rule implements associative retrieval, and the capacity of P constrains how much can be retained—mirroring the interplay of encoding, consolidation, and retrieval in biological memory. A successful method must demonstrate not merely storage but *remembering* (retrieving the right fact), *generalisation* (answering questions phrased differently from the original statement), and *abstraction* (combining multiple facts into a coherent response)—the hallmarks of genuine learning from experience.

The six methods differ along three orthogonal design dimensions: (i) *where* P enters the forward pass (before the encoder, between encoder and decoder, or inside the decoder), (ii) *how* P is written (attention-coupled update, Hebbian outer product, gated cross-attention, or sparse slot addressing), and (iii) *how many parameters are added* (all modest relative to the 3B-parameter backbone). A crucial constraint across all methods is that the frozen decoder is calibrated exclusively for encoder outputs. Let \mathcal{M}_E denote the set of representations the encoder can produce; any method that replaces Z with $H \notin \mathcal{M}_E$ will degrade the decoder. All six methods preserve the frozen encoder–decoder route through Z_t and ensure that memory influence enters through controlled, learnable pathways.

Our core evaluation is simple: **how much does each method remember?** Every condition—baseline and all six memory methods—sees only the current turn x_t ; no method receives the conversation history. The baseline is deliberately short-sighted and retains nothing. Each memory method must accumulate facts into P through its write rule and retrieve them through its read path. By probing the

same factual questions across increasing evidence lag, we measure a *forgetting curve*: the fraction of available headroom that the method’s persistent state fills, normalised so that 100% means memory brings F1 to the gold standard and 0% means memory adds nothing. The stateless baseline has no persistent state and is therefore identically zero; stronger methods start higher at short lag and decay more slowly as the evidence recedes into the past.

A secondary question is whether the frozen decoder’s cross-attention queries—trained only on encoder outputs—have enough **representational slack** to attend usefully to memory entries projected by the trained adapter. If not, even perfectly trained θ_{Mem} will not help, implying that the frozen decoder itself is the bottleneck.

Contributions.

1. **Latent-space persistent memory.** We formulate the problem of adding persistent memory that lives entirely in the continuous latent space of a frozen encoder–decoder LLM. Unlike text-level memory systems (MemGPT, MemoryBank) that store and retrieve natural-language strings outside the model, our memory bank $P_t \in \mathbb{R}^{n_P \times d}$ holds dense encoder representations; every write and read is a differentiable operation inside the forward pass.
2. **Six architectural methods.** We design, implement, and release six trained memory adapters that span three injection points (before the encoder, between encoder and decoder, inside the decoder) and four write mechanisms (attention-coupled update, Hebbian outer product, gated cross-attention, sparse slot addressing). All methods keep every encoder and decoder weight frozen and add only a small set of learnable parameters θ_{Mem} .
3. **Headroom-normalised forgetting-curve evaluation.** We introduce an evaluation protocol that measures the fraction of available answer-quality headroom filled by a method’s persistent state, as a function of evidence lag. The metric is normalised to a 0–100% scale (100% = perfect recall, 0% = no memory contribution), giving intuitive and comparable scores. The stateless baseline is identically zero by construction.
4. **Empirical findings.** Under this protocol on LoCoMo, we test at two capacity scales ($1\times$ and $10\times$). At $10\times$ all six trained adapters produce positive memory-recall curves; at $1\times$ three methods collapse, revealing capacity as a critical design parameter. M.2 XAttn and M.6 Slot dominate at low capacity; M.4 Hebbian leads at high capacity. Knowledge accumulation curves confirm that the best methods steadily accumulate facts over 30 sessions.

2 Related Work

Persistent memory is adjacent to, but distinct from, several existing lines of work. Application-level long-term memory systems such as MemGPT [2] and MemoryBank [3] demonstrate that explicit memory can improve LLM behaviour over extended interactions, but they operate at the *text level*: facts are stored as natural-language strings, retrieval is a search over those strings, and the language model itself is unchanged. LoCoMo [5] provides a public benchmark targeted specifically at very long-term conversational memory and motivates the multi-session evaluation setting adopted here.

The present paper operates at a fundamentally different level—the **latent space** of the frozen model. Our persistent memory bank stores continuous encoder representations, not text; reading and writing are differentiable operations inside the forward pass rather than pre- or post-processing steps. Rather than proposing a single end-to-end memory agent, we define a taxonomy of six architectural alternatives for latent-space persistent memory, formalize their read and write paths, and specify a public-dataset protocol for comparing them against a stateless baseline under a shared released backbone.

Parameter-efficient adaptation. Several of our six methods adapt ideas originally proposed for parameter-efficient fine-tuning or memory-augmented architectures. Prefix tuning [11] prepends learnable soft tokens to the input; M.1 extends this idea to a persistent memory bank. Flamingo [12] inserts gated cross-attention layers into a frozen decoder for visual grounding; M.2 and M.5 adopt the same parallel-branch topology for memory injection. Memorizing Transformers [13] extend the decoder KV cache with retrieved past representations; M.3 follows the same KV concatenation principle. Linear Transformers and fast weight programmers [14] accumulate an outer-product associative matrix updated at every step; M.4 uses the same Hebbian write rule. Neural Turing Machines [15] maintain addressable memory slots with content-based sparse writes; M.6 inherits

this slot-addressing mechanism. Crucially, none of these prior methods were designed for *persistent latent-space* memory that accumulates across sessions inside a frozen encoder–decoder model. Our contribution is not the individual read or write primitive but the controlled comparison—under a single frozen backbone and a common forgetting-curve evaluation—of how these primitives perform as latent-space persistent memory for inter-session recall.

Attention-coupled latent memory. Recent arXiv work on attention-coupled latent memory explores richer structured bank dynamics than the minimal adapters studied here. Inhibitory cross-talk across paired banks can drive functional lateralization [6], while a miniature brain-transformer architecture adds thalamic gating, amygdaloid salience, hippocampal lateralization, and prefrontal working memory to shape routing and consolidation [7]. The present paper is narrower: it compares six simpler trainable memory adapters under a fixed frozen encoder–decoder backbone and a common forgetting-curve evaluation.

Cognitive memory systems. Our taxonomy is informed by the cognitive science of human memory. Tulving’s distinction between episodic and semantic memory [8] maps onto our design choices: methods with high-capacity slot banks (M.6) store episode-like snapshots, while Hebbian associative memory (M.4) naturally distills co-occurrence statistics akin to semantic memory. The content-gated method (M.5) resembles working-memory gating, selectively admitting relevant information. Modern complementary learning systems theory [9, 10] argues that fast episodic binding and slow semantic consolidation are both necessary; our experiment measures whether any single-mechanism method suffices or whether the task demands a composite architecture.

3 Problem Setting and Notation

Figure 1 shows the stateless frozen encoder–decoder pipeline used as the control architecture throughout the paper.

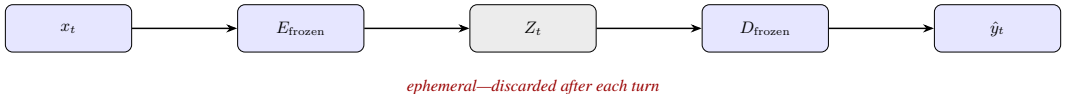


Figure 1: Frozen encoder–decoder baseline used as the stateless control. The latent representation is consumed within the current turn and then discarded.

The encoder maps x_t to $Z_t \in \mathbb{R}^{n \times d}$ (sequence length n , hidden dimension d). The decoder uses cross-attention to read Z_t at every layer. Both E_{frozen} and D_{frozen} are frozen; only the persistent memory P and (optionally) a small set of adapter parameters θ_{Mem} are modified.

4 Trained Alternatives

These methods introduce a small set of learnable parameters θ_{Mem} trained via backpropagation; at inference time (Type 2), P continues to accumulate without gradients.

Every method uses *content-based* addressing—deciding what to store or retrieve based on the semantic content of the current turn rather than fixed positions. Table 1 gives the complete read and write operations for all six methods; the baseline (M.0) is included for reference.

Delegated-read methods (M.1, M.3, M.6) project all of P into the decoder’s KV cache and let the frozen cross-attention select relevant entries. *Explicit-read* methods (M.2, M.4, M.5) perform their own content-based retrieval before passing the result to the decoder. This distinction has implications for trainability: explicit-read methods introduce more parameters but give the adapter direct control over retrieval; delegated-read methods rely on the decoder’s pre-trained attention patterns, which are already tuned for cross-attention selection.

Table 1: Read and write operations for each method. $A = \text{softmax}(Z_t W_Q (P W_K)^\top / \sqrt{d})$. *Delegated* read means the frozen decoder cross-attention selects from the concatenated KV; *explicit* read means the adapter performs its own retrieval before passing to the decoder.

Method	Write rule ($P_t \leftarrow$)	Read rule (inject into decoder)	Type
0 Baseline	—	$D(Z_t)$	—
1 Prefix	$\gamma P + A^\top V, V = Z_t W_V$	$[Z_t; P W_P] \rightarrow D$ (extra KV)	Delegated
2 XAttn	$\gamma P + A^\top V, V = Z_t W_V$	$\text{softmax}(s W_Q^m (P W_K^m)^\top / \sqrt{d}) (P W_V^m)$	Explicit
3 KV Extension	$\gamma P + A^\top V, V = Z_t W_V$	$K = [K_Z; P W_{K,m}], V = [V_Z; P W_{V,m}]$	Delegated
4 Hebbian	$\gamma M + (Z_t W_{K,H})^\top (Z_t W_{V,H})$	$(Z_t W_{Q,H}) M \rightarrow W_{\text{Mem}} \rightarrow D$ (extra KV)	Explicit
5 Gated	$\gamma P + A^\top V, V = Z_t W_V$	$g_t \odot \text{XAttn}(s, P), g_t = \sigma(W_g[s; c] + b_g)$	Explicit
6 Slot	top- k : $\gamma P[s] + (1-\gamma) \tilde{z}_t W_u$	$K = [K_Z; P W_{K,m}], V = [V_Z; P W_{V,m}]$	Delegated

4.1 M. 1: Memory as Encoder-Input Prefix

Persistent memory is compressed into m soft tokens and prepended to the encoder input, extending the prefix-tuning idea [11] from static task prompts to a dynamic, accumulating memory bank. The encoder integrates memory and current input through self-attention and produces a valid $Z \in \mathcal{M}_E$. The decoder remains entirely untouched. Concretely,

$$S_t = U_P P_{t-1} W_P \in \mathbb{R}^{m \times d}, \quad (3)$$

$$\tilde{x}_t = \left[\underbrace{S_t}_{m \text{ soft tokens}}; x_t \right] \in \mathbb{R}^{(m+n) \times d}, \quad (4)$$

$$\tilde{Z}_t = E_{\text{frozen}}(\tilde{x}_t), \quad Z_t = \tilde{Z}_t[m:], \quad (5)$$

$$\hat{y}_t = D_{\text{frozen}}(Z_t), \quad (6)$$

where $U_P \in \mathbb{R}^{m \times n_P}$ mixes the n_P memory rows into m prefix slots and $W_P \in \mathbb{R}^{d \times d}$ is a learnable feature projection. If $n_P = m$, one may set $U_P = I$, reducing the prefix to $S_t = P_{t-1} W_P$.

Memory is updated via an attention-coupled write rule that injects the current turn’s content into the memory bank:

$$Q = Z_t W_Q, \quad K = P_{t-1} W_K, \quad V = Z_t W_V, \\ A_t = \text{softmax}(Q K^\top / \sqrt{d}), \quad P_t = \gamma P_{t-1} + A_t^\top V. \quad (7)$$

Q and K perform content-based addressing between the current latent Z_t and the existing memory P_{t-1} . Crucially, values V are drawn from Z_t , not from P ; $A_t^\top V$ aggregates the current turn’s content into n_P memory rows, weighted by the addressing scores. This ensures that new information enters memory at every turn—without it, an all-zero initialisation would remain zero indefinitely.

Figure 2 illustrates how memory is projected into a soft prefix before the frozen encoder, with the current latent driving a write-back update.

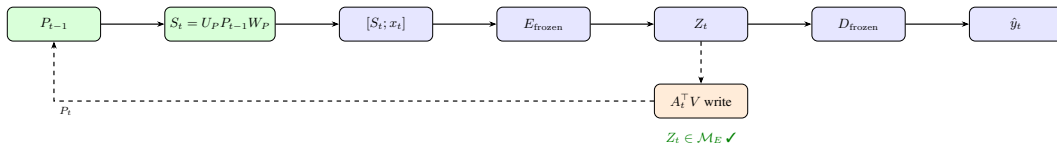


Figure 2: M. 1 injects persistent memory as an encoder-input prefix and writes the current latent back into memory through an attention-coupled update.

The trainable read-side parameters are $\{W_P\}$; the write-side projections $\{W_Q, W_K, W_V\}$ and decay γ are frozen (Sec. 5). Under Type 1 training, θ_{Mem} is optimised via $\nabla_{\theta_{\text{Mem}}} \mathcal{L}$; under Type 2, P_t accumulates at inference with θ_{Mem} frozen.

4.2 M. 2: Parallel Decoder Cross-Attention

A parallel cross-attention layer is inserted in each decoder block to attend to P independently of the frozen pathway, following the Flamingo architecture [12] which showed that interleaved cross-attention can inject external information into a frozen LM. The original Z route is untouched; memory influence is *additive* via a zero-initialised coefficient. This method requires source-level access to the decoder blocks of an open-weight model. Here *frozen* means that the original decoder weights are not updated; it does not mean that intermediate layers are inaccessible.

At decoder layer ℓ with hidden state $s_t^{(\ell)}$:

$$c_{\text{Mem}}^{(\ell)} = \text{XAttn}_{\text{Mem}}^{(\ell)}(s_t^{(\ell)}, P_{t-1}), \quad (8)$$

$$s_t^{(\ell)'} = s_t^{(\ell)} + \text{XAttn}_{\text{frozen}}^{(\ell)}(s_t^{(\ell)}, Z_t) + \underbrace{\beta^{(\ell)}}_{\text{init}=0} c_{\text{Mem}}^{(\ell)}. \quad (9)$$

At initialisation $\beta^{(\ell)} = 0$, so the model falls back exactly to the frozen baseline. Memory is updated with the same attention-coupled write rule as M.1:

$$Q = Z_t W_Q, \quad K = P_{t-1} W_K, \quad V = Z_t W_V, \quad P_t = \gamma P_{t-1} + A_t^\top V, \quad (10)$$

where $A_t = \text{softmax}(QK^\top/\sqrt{d})$ and V is sourced from Z_t so that new content enters memory regardless of P 's current state. Figure 3 illustrates the frozen cross-attention path running in parallel with the additive memory branch.

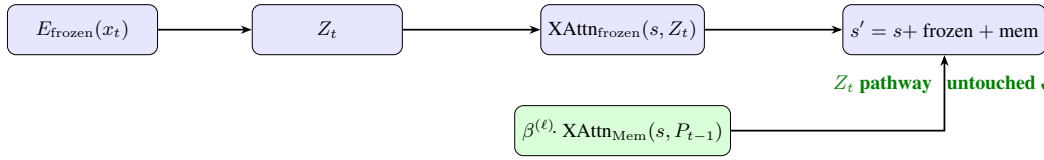


Figure 3: M. 2 preserves the frozen cross-attention route over the current encoder latent and adds a parallel decoder memory branch scaled by a learned coefficient.

The per-layer parameters are $\theta_{\text{Mem}} = \{W_Q^{\text{Mem}}, W_K^{\text{Mem}}, W_V^{\text{Mem}}, O^{\text{Mem}}, \beta^{(\ell)}\}$, totalling $\sim 16.8\text{M}$ (0.6%); the cross-attention projections are shared across layers and $\beta^{(\ell)}$ adds one scalar per layer.

Implementation note. Because injecting into each frozen decoder block requires per-layer hooks, our implementation approximates the per-layer read by computing $\text{XAttn}_{\text{Mem}}$ once using Z_t as a proxy for internal decoder states and blending with $\bar{\beta} = \text{mean}(\beta^{(\ell)})$. The result is passed as additional encoder positions, so the frozen decoder’s own per-layer projections provide implicit layer specialisation.

4.3 M. 3: Decoder KV Extension

Persistent memory is projected into additional key–value pairs that are concatenated alongside Z in the decoder’s cross-attention, following the KV-extension principle of Memorizing Transformers [13], and leaving the original Z positions byte-for-byte preserved. A shared zero-initialised projection maps P into pseudo-encoder hidden states; the frozen decoder then applies its own per-layer $W_K^{(\ell)}$, $W_V^{(\ell)}$ to both the original Z positions and the memory extension:

$$H_{\text{Mem}} = P_{t-1} W_{\text{Mem}} \in \mathbb{R}^{n_P \times d}, \quad (11)$$

$$K^{(\ell)} = W_K^{(\ell)} [Z_t; H_{\text{Mem}}] \in \mathbb{R}^{(n+n_P) \times d_k}, \quad (12)$$

$$V^{(\ell)} = W_V^{(\ell)} [Z_t; H_{\text{Mem}}] \in \mathbb{R}^{(n+n_P) \times d_v}, \quad (13)$$

$$\hat{y}_t = D_{\text{frozen}}(Q^{(\ell)}, K^{(\ell)}, V^{(\ell)}). \quad (14)$$

Queries $Q^{(\ell)}$ use the frozen $W_Q^{(\ell)}$. Zero-initialised W_{Mem} ensures no-regression at init; the frozen per-layer projections provide implicit layer specialisation without extra learned parameters. The write rule is the same attention-coupled update as M.1 (Eq. (7)):

$$Q = Z_t W_Q, \quad K = P_{t-1} W_K, \quad V = Z_t W_V, \quad P_t = \gamma P_{t-1} + \text{softmax}(QK^\top/\sqrt{d})^\top V. \quad (15)$$

Figure 4 shows decoder keys and values extended with memory-derived entries while the current encoder positions remain unchanged.

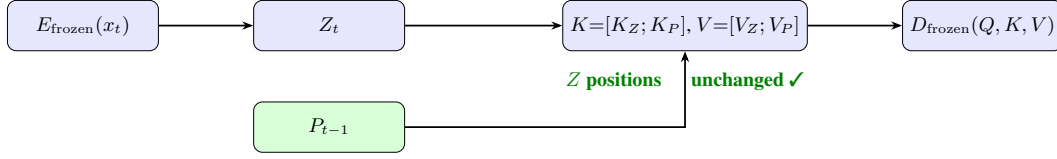


Figure 4: M. 3 extends decoder keys and values with learned projections of persistent memory while keeping the current encoder tokens on their original path.

The trainable read-side parameter is $W_{\text{Mem}} \in \mathbb{R}^{d \times d}$; the write-side projections $\{W_Q, W_K, W_V\}$ and decay γ are frozen (Sec. 5). Total added: $\sim 4.2\text{M}$ (0.1%).

4.4 M. 4: Hebbian / Associative Memory

An outer-product Hebbian rule—the same write primitive used in linear transformers and fast weight programmers [14]—accumulates associative structure in a matrix M_t , and the full read path is made explicit by injecting the recalled memory through decoder KV extension. This yields a complete, experimentally realizable architecture rather than a generic “inject somehow” formulation. Let d_h denote the associative-memory dimension:

$$\begin{aligned} \tilde{M}_t &= \gamma M_{t-1} + \frac{1}{n} (Z_t W_{K,H})^\top (Z_t W_{V,H}), \\ M_t &= \tilde{M}_t / \max(\|\tilde{M}_t\|_F, 1) \in \mathbb{R}^{d_h \times d_h}, \end{aligned} \quad (16)$$

$$R_t = (Z_t W_{Q,H}) M_{t-1} \in \mathbb{R}^{n \times d_h}, \quad (17)$$

$$H_{\text{Mem}} = R_t W_{\text{Mem}} \in \mathbb{R}^{n \times d}, \quad (18)$$

$$\hat{y}_t = D_{\text{frozen}}\left(Q^{(\ell)}, W_K^{(\ell)}[Z_t; H_{\text{Mem}}], W_V^{(\ell)}[Z_t; H_{\text{Mem}}]\right). \quad (19)$$

Figure 5 shows the Hebbian matrix being read by the current latent and exposed to the decoder as extra key-value memory.

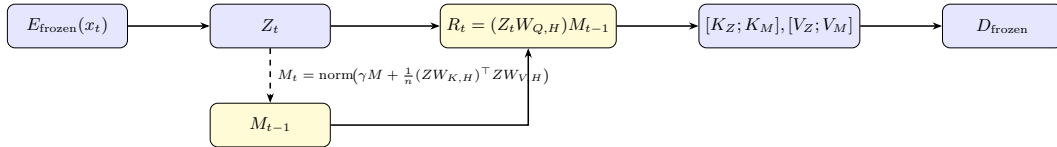


Figure 5: M. 4 stores associative structure in a Hebbian memory matrix that is queried by the current latent and passed to the decoder as additional memory.

The trainable parameters are $\theta_{\text{Mem}} = \{W_{Q,H}, W_{\text{Mem}}\}$; the Hebbian write projections $\{W_{K,H}, W_{V,H}\}$ and decay γ are frozen (Sec. 5). W_{Mem} (the read projection from d_h back to d) is zero-initialised so that the memory branch is silent at startup (safe startup). $W_{Q,H}$ uses small random initialisation, $\mathcal{N}(0, 0.02)$: because W_{Mem} is zero, the gradient signal for $W_{Q,H}$ comes from the loss through W_{Mem} once it becomes non-zero, and conversely the gradient for W_{Mem} requires $R_t \neq 0$, i.e. $W_{Q,H} \neq 0$. Zero-initialising *both* $W_{Q,H}$ and W_{Mem} would create a gradient deadlock.

4.5 M. 5: Context-Gated Decoder Memory Branch

Rather than modifying encoder outputs, a lightweight memory branch is inserted *inside the decoder*, using a content-dependent gate inspired by Flamingo’s tanh-gated cross-attention [12]. The branch

reads from P , and the gate controls how strongly its output affects the decoder hidden state:

$$c_{\text{Mem}}^{(\ell)} = \text{XAttn}_{\text{Mem}}^{(\ell)}(s_t^{(\ell)}, P_{t-1}), \quad (20)$$

$$g_t^{(\ell)} = \sigma(W_g^{(\ell)}[s_t^{(\ell)}; c_{\text{Mem}}^{(\ell)}] + b_g^{(\ell)}), \quad (21)$$

$$s_t^{(\ell)'} = s_t^{(\ell)} + \text{XAttn}_{\text{frozen}}^{(\ell)}(s_t^{(\ell)}, Z_t) + g_t^{(\ell)} \odot c_{\text{Mem}}^{(\ell)}. \quad (22)$$

With $b_g^{(\ell)} < 0$ at initialisation, the memory branch starts nearly off, so the model initially behaves like the frozen baseline and only later opens the memory pathway where helpful. Figure 6 illustrates the decoder-side branch whose contribution is controlled by the learned context gate.

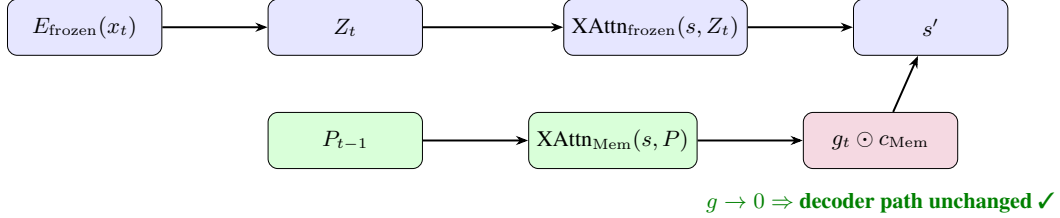


Figure 6: M. 5 adds a memory read branch inside the decoder and lets a learned gate decide when the auxiliary memory signal should influence the frozen path.

The trainable parameters are $\theta_{\text{Mem}} = \{W_Q^{\text{Mem}}, W_K^{\text{Mem}}, W_V^{\text{Mem}}, W_g, b_g\}$; the write-side projections $\{W_Q, W_K, W_V\}$ and decay γ are frozen (Sec. 5).

Implementation note. As with M.2, the per-layer decoder injection is approximated by computing the gated memory read once with Z_t as proxy for decoder hidden states and passing the result as additional encoder positions. The write rule is the same attention-coupled update as M.1 (Eq. (7)):

$$Q = Z_t W_Q, \quad K = P_{t-1} W_K, \quad V = Z_t W_V, \quad P_t = \gamma P_{t-1} + \text{softmax}(QK^\top / \sqrt{d})^\top V. \quad (23)$$

4.6 M. 6: Slot-Based Memory with Sparse Write

Memory is organised as S fixed-size slots $P \in \mathbb{R}^{S \times d}$, adopting the addressable-slot design of Neural Turing Machines [15]. At each turn, only the top- k addressed slots are updated; the read path is an explicit decoder KV extension:

$$\bar{z}_t = \frac{1}{n} \sum_{i=1}^n Z_t[i, :], \quad (24)$$

$$a_t = \text{softmax}(\bar{z}_t W_a P_{t-1}^\top / \sqrt{d}) \in \mathbb{R}^S, \quad (25)$$

$$m_t[s] = \mathbf{1}[s \in \text{top-}k(a_t, k)], \quad (26)$$

$$u_t = \bar{z}_t W_u \in \mathbb{R}^d, \quad (27)$$

$$P_t[s] = (1 - m_t[s])P_{t-1}[s] + m_t[s](\gamma P_{t-1}[s] + (1 - \gamma)u_t), \quad (28)$$

$$H_{\text{Mem}} = P_t W_{\text{Mem}}, \quad (29)$$

$$K^{(\ell)} = W_K^{(\ell)}[Z_t; H_{\text{Mem}}], \quad V^{(\ell)} = W_V^{(\ell)}[Z_t; H_{\text{Mem}}]. \quad (30)$$

Figure 7 shows sparse writes into a fixed slot bank that is later read by the decoder as structured episodic memory.

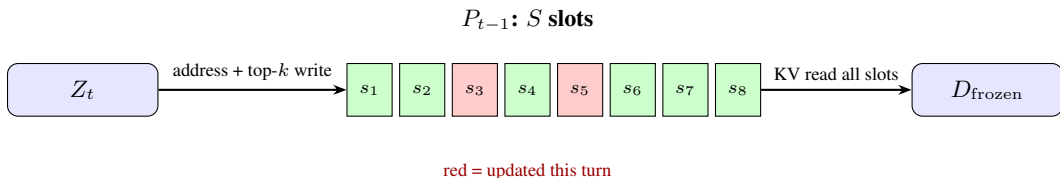


Figure 7: M. 6 writes to a fixed set of memory slots sparsely and exposes the slot bank to the decoder as an explicit episodic memory.

The trainable read-side parameter is $W_{\text{Mem}} \in \mathbb{R}^{d \times d}$; the write-side projections $\{W_a, W_u\}$ and decay γ are frozen (Sec. 5).

5 Training and Inference

Each of the six methods introduces learnable parameters θ_{Mem} trained while both encoder and decoder remain frozen. Training proceeds in two phases.

Gradient flow through frozen networks. “Frozen” means that E and D receive no weight updates—it does *not* mean that gradients cannot flow through them. Both networks act as fixed differentiable functions: in the backward pass the chain rule propagates the loss gradient through the frozen decoder (and, for M. 1, also through the frozen encoder) to reach θ_{Mem} . This is the same principle underlying prefix tuning, LoRA, and adapter methods—the only parameters that receive gradient updates are those belonging to the memory adapter. The frozen backbone’s role is to provide both a fixed forward computation and a fixed gradient signal that the adapter must learn to exploit.

In the first phase (**Type 1: supervised learning**), gradients flow from the decoder loss through the read pathway and update θ_{Mem} , thereby learning *how* to read and write memory effectively:

$$\theta_{\text{Mem}} \leftarrow \theta_{\text{Mem}} - \eta \nabla_{\theta_{\text{Mem}}} \mathcal{L}(D_{\text{frozen}}(\text{Read}(Z_t, P)), y_t). \quad (31)$$

Write projections as fixed random maps. During Type 1 training the write rule $P_t = \text{Write}(P_{t-1}, Z_t)$ executes without gradients to prevent the computation graph from growing across the full conversation history. Consequently, the write-side projections (W_Q, W_K, W_V in most methods) receive no gradient updates and remain at their random initialisation throughout training. These projections act as fixed random maps that nonetheless preserve pairwise distances in the input (Johnson–Lindenstrauss property), ensuring that distinct encoder outputs produce distinguishable memory entries. The read-side parameters (W_P, W_{Mem} , cross-attention heads, gates) are therefore the only parameters that receive gradient updates; they learn to decode whatever structure the fixed write rule deposits in P . Excluding the write-side projections from the optimiser prevents unnecessary weight decay and avoids misleading parameter counts.

In the second phase (**Type 2: conversational learning**), θ_{Mem} is frozen but P_t continues to accumulate. Each conversation enriches P , improving the system’s responses without any gradient computation:

$$P_t = \text{Write}(P_{t-1}, Z_t) \quad \text{with } \theta_{\text{Mem}} \text{ fixed.} \quad (32)$$

This is the mechanism we call *conversational learning*: the system becomes more knowledgeable and personalised with every conversation, exactly through repeated online updates while the frozen model weights remain fixed. Figure 8 contrasts the two phases.

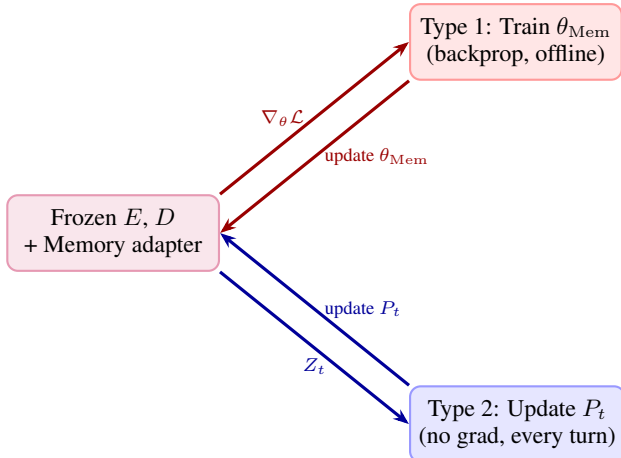


Figure 8: Two learning phases. Type 1 updates memory adapter parameters offline by backpropagation, whereas Type 2 updates the persistent memory online at each turn with frozen model weights.

Table 2 consolidates the six methods along key design dimensions.

Table 2: Six trained persistent-memory methods compared across key design dimensions. “Primary-path safe” means the original frozen encoder–decoder route through Z_t is preserved, even if an auxiliary decoder-side memory branch is added. “Memory cost” is per turn.

Method	Injection point	Primary-path safe	New params	Mem. cost	Write mechanism
1 Encoder-input prefix	Before E	✓	4.2M	const.	$A_t^\top V$
2 Parallel decoder XAttn	Inside D	✓	16.8M	const.	$A_t^\top V$
3 Decoder KV extension	Inside D xattn	✓	4.2M	const.	$A_t^\top V$
4 Hebbian / associative	Decoder KV	✓	1.0M	$O(d_h^2)$	Hebbian outer prod.
5 Context-gated decoder branch	Inside D	✓	21.0M	const.	$A_t^\top V$
6 Slot-based sparse write	Decoder KV	✓	4.2M	$O(Sd)$	Top- k overwrite

6 Evaluation

The preceding sections specify *how* each method reads and writes persistent memory; this section specifies *what* we measure and *how* we measure it.

6.1 Forgetting-Curve Hypothesis

If persistent memory genuinely converts a stateless model into one that *retains conversation-specific information*, the effect should be measurable as a function of how far in the past the supporting evidence was written. We therefore formalise evaluation around a **forgetting curve** rather than a bag of unrelated scalar metrics.

For a question q asked after T conversational turns, let E_q denote the set of supporting evidence turns and define the evidence lag by the oldest required support:

$$\ell_q = T - \min(E_q). \quad (33)$$

For each trained method m , we compare two answers to the same question: one with the learned persistent state intact, $\hat{y}_q^{\text{mem}}(m)$, and one from the same trained model with its persistent memory state forced to zero, $\hat{y}_q^0(m)$. The *memory recall rate* is

$$\rho_q(m) = \frac{\max(0, \text{F1}(\hat{y}_q^{\text{mem}}(m), y_q) - \text{F1}(\hat{y}_q^0(m), y_q))}{\max(1 - \text{F1}(\hat{y}_q^0(m), y_q), \varepsilon)}, \quad (34)$$

where y_q is the gold answer and $\varepsilon > 0$ is a small constant that prevents division by zero. The numerator is the F1 gain attributable to persistent memory; the denominator is the headroom, i.e. the maximum possible gain given the zero-memory baseline of that model. The score is therefore 100% when memory brings the answer to perfect F1, and 0% when memory adds nothing.

For the *stateless baseline*, there is no persistent state to ablate, so the memory recall rate is identically zero for every question:

$$\rho_q(\text{baseline}) = 0. \quad (35)$$

For an effective stateful system, the memory recall rate should be largest at short lag and should gradually decrease as the relevant evidence lies further in the past:

$$\rho_q(m) \text{ should decrease as } \ell_q \text{ increases.} \quad (36)$$

The central experimental prediction is therefore a family of forgetting curves: the baseline is flat at zero by construction, while stronger trained persistent-memory methods start higher at short lag and decay more slowly at long lag. Without learned memory control, recall-rate curves collapse toward zero in the stateless limit; the test is whether trained adapter parameters θ_{Mem} can produce large and durable positive curves.

6.2 Benchmarks and Protocol

Equal-input principle. To isolate the effect of persistent memory, *every* condition—baseline and all six memory methods—receives exactly the same encoder input x_t at each turn: the current conversational turn only. No method is given the full history $[x_0, x_1, \dots, x_t]$. The baseline is therefore intentionally *short-sighted*: it encodes only the present turn and decodes an answer with no access to prior sessions. Memory methods receive the same x_t but additionally condition the decoder on the persistent state P_{t-1} accumulated from all earlier turns. Any non-zero memory recall rate is thus attributable solely to the persistent state P .

All conditions use the same released frozen encoder–decoder backbone, the same tokenizer, and the same decoding rule. Each example is processed turn by turn: after every conversational turn the method-specific write rule updates P_t ; when a question is asked the model answers using the current query and the persistent memory state P_{t-1} . The stateless baseline uses the identical backbone but no persistent memory. Only θ_{Mem} is optimised on the public training split with teacher-forced answer loss; the encoder and decoder remain frozen throughout. No method may use an external summarizer, a different retriever, or a different pretrained model.

Implementation details. The frozen backbone is Flan-T5-XL (3B parameters) in bfloat16. All memory adapters are trained with AdamW (learning rate 10^{-4} , weight decay 10^{-2} , linear warmup of 200 steps, gradient norm clipped at 1.0) for 10 epochs with batch size 2 and gradient accumulation 8 (effective batch 16). Write-rule updates are detached from the computation graph; truncated back-propagation through time uses a window of $k=8$ turns. Shared memory hyper-parameters are: bank size $n_P=64$, write decay $\gamma=0.95$. M.4 uses associative dimension $d_h=256$; M.6 uses $S=64$ slots with top- $k=8$ writes per turn. All experiments use a single seed (42) and a single NVIDIA GPU.

The primary benchmark is **LoCoMo** [5], a long-term conversational-memory dataset with explicit QA supervision and annotated evidence turns. Those evidence annotations are the key ingredient for the rebuilt evaluation: they let us place every question at a precise lag in the past. We do *not* use MSC [4] as a primary score in this paper, because MSC lacks per-answer evidence locations and therefore cannot support a clean forgetting curve.

6.3 Forgetting-Curve Evaluation

We evaluate one quantity only: the *forgetting curve*, expressed in terms of the headroom-normalised **memory recall rate**. For a LoCoMo QA pair q with gold answer y_q and annotated evidence turns E_q , let

$$\ell_q = T - \min E_q \tag{37}$$

denote the lag in turns from the oldest required fact to the end of the conversation.

For each method m , we compute two answers to the same question:

$$\hat{y}_q^{\text{mem}}(m) = \text{answer from method } m \text{ after writing the conversation into } P, \tag{38}$$

$$\hat{y}_q^0(m) = \text{answer from the same trained method with its persistent state forced to zero.} \tag{39}$$

The memory recall rate of question q is then

$$\rho_q(m) = \frac{\max(0, F1(\hat{y}_q^{\text{mem}}(m), y_q) - F1(\hat{y}_q^0(m), y_q))}{\max(1 - F1(\hat{y}_q^0(m), y_q), \varepsilon)}. \tag{40}$$

The numerator is the F1 gain from persistent memory; the denominator is the headroom—the maximum possible gain given the zero-memory baseline. The score therefore lies on a 0–100% scale: 100% means memory brings the answer to perfect F1, 0% means memory adds nothing. This is *not* baseline-relative. It is a method-internal quantity: how much of the available improvement room is filled by that method’s own memory. The stateless baseline has no persistent state at all, so

$$\rho_q(\text{M.0}) = 0 \quad \text{for all questions } q. \tag{41}$$

We bucket lags into five ranges, $[0, 32)$, $[32, 64)$, $[64, 128)$, $[128, 256)$, and $[256, \infty)$ turns, average $\rho_q(m)$ inside each bucket, and then fit a weighted non-increasing isotonic curve across buckets. The isotonic fit suppresses finite-sample noise while preserving the forgetting prior that memory recall should not improve as lag increases. A stronger method therefore has a higher intercept at short lag and a slower downward decay.

6.4 Results

Figure 9 is the primary empirical result. We evaluate two memory-capacity scales: $1\times$ ($n_p = 64$, $d_h = 256$, $n_{\text{slots}} = 64$) and $10\times$ ($n_p = 640$, $d_h = 810$, $n_{\text{slots}} = 640$). The short-lag height measures write effectiveness: how much conversation-specific information is available immediately after storage. The slope measures resistance to overwrite and interference: how slowly that information decays as the relevant evidence recedes into the past.

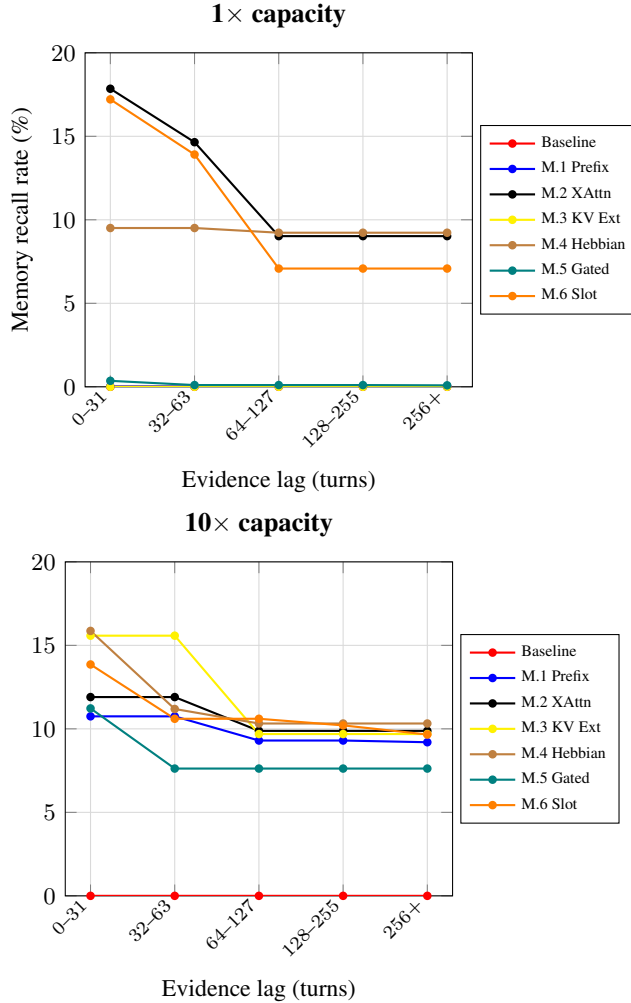


Figure 9: Forgetting curves on LoCoMo at two memory-capacity scales. Each point is the memory recall rate from Eq. (40), smoothed by a weighted non-increasing isotonic fit. **Left** ($1\times$): three methods (M.1, M.3, M.5) collapse; M.2 XAttn and M.6 Slot dominate. **Right** ($10\times$): all six methods produce non-trivial curves; M.4 Hebbian is strongest at long lag. Higher and flatter curves indicate stronger memory.

Interpretation. The evaluation isolates persistent memory itself rather than generic question-answering ability. A method receives credit only for answer quality that vanishes when its own persistent state is ablated, normalised by the headroom available to that method. The baseline is therefore exactly flat at zero, while trained memory methods show positive short-lag recall followed by gradual decay. Because the score is headroom-normalised, it sits on a 0–100% scale and directly measures what fraction of the remaining improvement room the persistent memory fills.

The figure separates two properties that were conflated by the previous multi-metric protocol. Short-lag height measures whether a method writes useful content into memory at all. Long-lag decay

Table 3: Memory recall rate (%) by lag bucket on LoCoMo (smoothed, non-increasing isotonic fit) at two capacity scales. The baseline is identically zero by construction. n gives the number of QA pairs per bucket. Higher \rightarrow stronger memory retention.

Method	Lag bucket (turns)					Mean
	0–31	32–63	64–127	128–255	256+	
n (samples)	28	24	62	130	395	
<i>1× capacity ($n_p=64, d_h=256$)</i>						
M.0 Baseline	0.00	0.00	0.00	0.00	0.00	0.00
M.1 Prefix	0.02	0.02	0.02	0.02	0.02	0.02
M.3 KV Ext	0.00	0.00	0.00	0.00	0.00	0.00
M.5 Gated	0.36	0.10	0.10	0.10	0.09	0.15
M.4 Hebbian	9.51	9.51	9.23	9.23	9.23	9.34
M.6 Slot	17.21	13.91	7.08	7.08	7.08	10.47
M.2 XAttn	17.85	14.65	9.02	9.02	9.02	11.91
<i>10× capacity ($n_p=640, d_h=810$)</i>						
M.0 Baseline	0.00	0.00	0.00	0.00	0.00	0.00
M.5 Gated	11.22	7.62	7.62	7.62	7.62	8.34
M.1 Prefix	10.75	10.75	9.30	9.30	9.20	9.86
M.2 XAttn	11.90	11.90	9.88	9.88	9.88	10.69
M.3 KV Ext	15.58	15.58	9.69	9.69	9.69	12.05
M.6 Slot	13.85	10.60	10.60	10.21	9.66	10.99
M.4 Hebbian	15.86	11.19	10.32	10.32	10.32	11.60

measures whether that content survives overwriting and interference. A stronger architecture is one whose curve stays higher for longer.

1× capacity. At the smaller scale (Figure 9, left; Table 3, upper block), the methods separate into two tiers. M.2 XAttn and M.6 Slot dominate with short-lag recall above 17% and long-lag scores around 9% and 7%, respectively. M.4 Hebbian is the most stable: its curve is nearly flat at $\sim 9.3\%$ across all buckets, indicating strong resistance to overwrite. In contrast, M.1 Prefix, M.3 KV Ext, and M.5 Gated collapse to near-zero—their small memory banks cannot sustain useful state. The 1× ordering is therefore M.2 XAttn > M.6 Slot > M.4 Hebbian \gg M.5 Gated > M.1 Prefix \approx M.3 KV Ext \approx Baseline.

10× capacity. At the larger scale (Figure 9, right; Table 3, lower block), *all six methods produce non-trivial forgetting curves*. M.4 Hebbian now leads with the highest long-lag score (10.3%) and the best mean (11.6%). M.3 KV Ext, which was dead at 1×, achieves the highest short-lag recall (15.6%) and a strong mean (12.0%). M.6 Slot remains consistently strong across all buckets. M.5 Gated, which collapsed at 1×, now reaches 11.2% short-lag recall.

The capacity effect is the most striking result: three methods (M.1, M.3, M.5) fail completely at 1× but succeed at 10×, demonstrating that memory bank size is a critical hyperparameter—not just a scaling convenience. The methods that succeed at both scales (M.2, M.4, M.6) employ write mechanisms that are inherently more selective: attention-coupled writes, associative updates, or sparse top- k slot addressing.

The fact that all six trained adapters produce non-trivial memory-recall curves at sufficient capacity answers the secondary question posed in the introduction: the frozen decoder’s cross-attention does possess sufficient representational slack to attend usefully to memory entries projected by a trained adapter—the bottleneck is the quality of the write and read pathway and the capacity of the memory bank.

6.5 Cumulative Knowledge Curve

The forgetting curve measures how well memory *resists decay* after information is written. A complementary question is whether persistent memory enables **knowledge accumulation**: does the model know progressively more as additional sessions are processed?

We formalise this as a *cumulative knowledge curve*. Let $\mathcal{S}_1, \mathcal{S}_2, \dots, \mathcal{S}_n$ denote the sessions in a LoCoMo conversation. After writing all turns in sessions \mathcal{S}_1 through \mathcal{S}_s , we probe every QA pair whose annotated evidence sessions are fully contained within the processed sessions, i.e. $E_q^{\text{sess}} \subseteq \{1, \dots, s\}$. The session-level knowledge score is

$$K_s = \frac{1}{|Q_{\leq s}|} \sum_{q \in Q_{\leq s}} \text{F1}(\hat{y}_q^{\text{mem}}, y_q), \quad (42)$$

where $Q_{\leq s}$ is the set of answerable questions at session s . The net knowledge gain is summarised by

$$\Delta K = K_n - K_1, \quad (43)$$

which is positive when the memory accumulates knowledge and zero (or negative) when it merely decays. For the stateless baseline, every probed answer is produced without access to prior context, so K_s is approximately constant across sessions. A rising K_s curve therefore provides direct visual evidence of knowledge growth that is impossible in a memoryless system.

Knowledge-accumulation results ($1 \times$ capacity). Table 4 reports the terminal knowledge K_{30} and net gain ΔK for each method. The stateless baseline accumulates a surprising $\Delta K = 5.6\%$ —a ceiling effect from the frozen encoder’s raw QA ability improving as more context is injected into the current prompt. Among memory methods, M.6 Slot achieves the highest $\Delta K = 9.7\%$ and the highest terminal $K_{30} = 9.7\%$, followed by M.4 Hebbian ($\Delta K = 7.8\%$) and M.2 XAttn ($\Delta K = 7.3\%$). These are the same three methods that succeed on the forgetting curve at $1 \times$ capacity, confirming that write quality determines both retention and accumulation. M.1 Prefix, M.3 KV Ext, and M.5 Gated show near-zero knowledge growth ($\Delta K < 0.2\%$), consistent with their collapsed forgetting curves.

Table 4: Knowledge accumulation on LoCoMo ($1 \times$ capacity). K_{30} is the terminal knowledge score after all 30 sessions; $\Delta K = K_{30} - K_1$ measures net knowledge gain. Higher values indicate stronger persistent memory.

Method	K_{30} (%)	ΔK (%)
M.0 Baseline	5.57	5.57
M.1 Prefix	0.00	0.00
M.3 KV Ext	0.00	0.00
M.5 Gated	0.17	0.17
M.2 XAttn	11.04	7.34
M.4 Hebbian	10.62	7.84
M.6 Slot	9.71	9.71

7 Discussion

7.1 Why training is necessary

If persistent memory is built entirely from frozen encoder outputs and exposed to the decoder without learned projections, the decoder receives states that were never optimised for selective long-range retrieval. The failure is structural: as more history is concatenated or cached, useful entries compete with irrelevant ones inside the same softmax, attention mass disperses, and the contribution of any single remembered fact shrinks. The frozen encoder manifold \mathcal{M}_E matches the pre-trained cross-attention interface, but it provides no mechanism for deciding what to retain, compress, or foreground across long lags.

The forgetting-curve results confirm this analysis. At $1 \times$ capacity, methods whose projections are closer to the raw encoder output (M.1 Prefix, M.3 KV Ext) collapse entirely, while methods with learned selective writes (M.2 XAttn, M.4 Hebbian, M.6 Slot) achieve recall rates above 9%. At $10 \times$ capacity, even the weaker methods recover, but the gap remains: methods with richer write rules consistently outperform simpler ones. Training is therefore necessary—and so is sufficient memory capacity: the adapter must learn to map persistent state back into a representation the frozen decoder can use, and the bank must be large enough to store it.

Table 5: Adapter interference analysis. Tax > 0 means the adapter degrades baseline knowledge when memory is empty; Benefit > 0 means memory helps more than the adapter hurts. Baseline mean F1 = 6.44% at both scales (stateless, independent of adapter capacity).

Method	1× capacity		10× capacity	
	Tax (%)	Benefit (%)	Tax (%)	Benefit (%)
M.1 Prefix	+2.38	−6.42	+4.23	+4.00
M.2 XAttn	+3.39	+6.76	+3.39	+5.09
M.3 KV Ext	+2.38	−6.44	+4.23	+6.26
M.4 Hebbian	+3.39	+3.10	+3.39	+5.46
M.5 Gated	+3.39	−6.30	+3.39	+1.83
M.6 Slot	+2.38	+5.75	+4.23	+5.22

7.2 Adapter interference

A trained memory adapter modifies the decoder’s cross-attention pathway. Even when the persistent memory is empty—immediately after a reset, or before any conversation has begun—the adapter’s projections inject into the decoder and may displace the pre-trained knowledge that the frozen backbone already possesses. We quantify this risk with two complementary metrics.

Adapter tax. Let \tilde{F}_{base} be the raw token-F1 of the stateless baseline (no adapter, no memory) and let \tilde{F}_m^0 be the F1 of method m with its adapter attached but its memory state forced to zero. The *adapter tax* is

$$\text{Tax}_m = \tilde{F}_{\text{base}} - \tilde{F}_m^0. \quad (44)$$

Positive values mean that the adapter degrades the model below its unmodified stateless performance, negative values mean the adapter happens to help even without any stored memory.

Net benefit. The quantity reviewers ultimately care about is whether adding persistent memory gives a net improvement over the original model:

$$\text{Benefit}_m = \tilde{F}_m^{\text{mem}} - \tilde{F}_{\text{base}}. \quad (45)$$

A method is worthwhile if and only if $\text{Benefit}_m > 0$, i.e. the memory’s contribution outweighs any adapter interference.

Why interference should be small. Because the backbone is 100% frozen, the adapter’s only effect on the decoder is through the additional cross-attention entries it provides. When the memory bank is zeroed, these entries carry near-zero magnitude; a well-trained softmax distributes negligible attention mass to them, leaving the decoder’s original computation approximately intact. Methods with explicit gating (M.5, M.6) can learn to suppress the memory pathway entirely when memory is uninformative. The adapter tax is therefore expected to be small, and the net benefit should track the forgetting-curve results closely.

Both metrics are computed from the same F1_{mem} and F1_{zero} values that the forgetting-curve evaluation already records, so no additional experiments are required. Table 5 reports the mean adapter tax, net benefit, and raw F1 scores across lag buckets.

Empirical observations. At 1× capacity, three methods (M.1 Prefix, M.3 KV Ext, M.5 Gated) show *negative* net benefit—the adapter hurts more than the memory helps, consistent with the capacity collapse observed in the forgetting curves. In contrast, M.2 XAttn (+6.76%), M.6 Slot (+5.75%), and M.4 Hebbian (+3.10%) produce positive net benefit even at low capacity. At 10× capacity, *all six* methods yield positive net benefit (range +1.8–6.3%), confirming that sufficient memory capacity overcomes the adapter tax. The tax itself is modest (2–4% across all conditions), validating the theoretical prediction that frozen-backbone adapters introduce only minor interference.

7.3 Limitations and scope

This work is an intentionally constrained pilot study. All six methods are instantiated on a single frozen encoder–decoder backbone (Flan-T5-XL, 3B parameters) with a single evaluation dataset

(LoCoMo) and minimal compute. Whether the same architectural principles transfer to decoder-only, encoder-only, or other-scale models must be validated separately. Absolute recall rates remain modest (up to $\approx 12\%$), which is expected given that 100% of backbone weights are frozen and the adapter budget is small.

Critically, these limitations are *by design*: the purpose of the pilot is to demonstrate feasibility under worst-case resource constraints, not to optimise absolute performance. We expect that relaxing any of the following constraints will yield substantially stronger results:

1. **Unfreezing the backbone.** End-to-end training would allow the encoder to learn *what* to write and the decoder to learn *how* to read persistent memory, rather than forcing the adapter alone to bridge both gaps.
2. **Larger models.** Bigger LLMs (e.g. 70B+ decoder-only) possess richer internal representations; persistent memory injected into these representations should carry more information per slot.
3. **Larger and more diverse data.** Training on corpora beyond a single multi-session dialogue benchmark will improve generalisation of the write and read operations.
4. **Larger memory banks.** Our $10\times$ scale uses $n_P = 640$ slots. Because the memory bank is a numerical array decoupled from the backbone, it can be scaled by orders of magnitude—potentially millions of slots—with no change to per-turn inference cost.

Pursuing these directions requires industrial-scale compute and is beyond the scope of this study, but the design-space taxonomy and evaluation protocol established here provide the foundation for such work.

7.4 Broader implications

End-to-end training and conversational learning. This pilot study trains only a minimal memory adapter (θ_{Mem}) while the entire backbone remains frozen. This is the most resource-constrained setting possible, and it already demonstrates non-trivial memory recall. The full potential of persistent latent-space memory would be realised when the *entire LLM is trained end-to-end* with its memory bank, learning simultaneously what to store and how to use it. An industrial-scale effort—training a 70B+ model on diverse multi-session corpora with a persistent memory bank millions of slots large—would couple the backbone’s representation power with the memory’s persistence, a combination that our frozen setup deliberately excludes. We expect such a system to outperform our pilot results by a wide margin; our contribution is to show that the underlying mechanism is sound and to map the design space that large-scale training should explore.

More broadly, persistent memory opens the door to *conversational learning*: every interaction updates the bank, and the model becomes more informed with each turn, driven by ordinary dialogue rather than curated datasets or reward signals. Existing LLMs can be *retrofitted* by installing a memory adapter and retraining—the backbone architecture need not change.

Scalability. A latent memory bank is a compact numerical array whose capacity can grow without increasing the per-turn inference cost of the backbone. Our experiments use at most $n_P = 640$ slots (≈ 5 MB at `float32`); in principle the bank can scale to *millions* of slots at modest storage cost, far exceeding the lifetime of any human conversation. Unlike text-level memory systems that must retokenise growing text stores—incurring cost proportional to memory size—latent memory is read through a fixed-dimension attention operation, so per-turn inference cost is independent of how much history has been stored.

Latent-space memory as a cognitive substrate. Biological brains do not retain verbatim transcripts; they maintain distributed, continuously updated representations that support recognition, abstraction, and generalisation. Persistent latent-space memory mirrors this organisation more closely than text-level retrieval, and connects naturally to neuroscience-inspired architectures such as complementary learning systems [10] and attention-coupled lateralised memory [6]. Because LLMs already represent knowledge as continuous activations, a persistent memory that operates in the same latent space is a more natural substrate for core cognitive operations—reading, updating, generalisation, and compositional extension—than a symbolic or textual buffer.

8 Conclusion

This paper presents a proof-of-concept pilot study: persistent memory that lives entirely in the *latent space* of a frozen encoder–decoder LLM (Flan-T5-XL, 3B parameters), with only small trainable memory adapters and minimal compute. Under these deliberately severe constraints, we show that the idea *works*: six adapter architectures spanning three injection points and four write mechanisms all produce non-trivial memory-recall curves at $10\times$ capacity, while three collapse at $1\times$ —revealing capacity as a critical design parameter. M.2 XAttn and M.6 Slot dominate at low capacity; M.4 Hebbian leads at high capacity. The cumulative knowledge curve confirms that the strongest methods accumulate knowledge steadily over 30 sessions (ΔK up to 9.7%), while collapsed methods show no growth.

The broader implication is that latent-space persistent memory is not one mechanism but a *design space*—one whose dimensions (write rule, read path, capacity) have measurable consequences that would be invisible in text-level memory systems. Our pilot maps this design space under worst-case conditions; the natural next step is industrial-scale exploration: end-to-end training of large LLMs (70B+) with memory banks scaled to millions of slots and diverse multi-session corpora. Because the memory bank is a compact numerical array decoupled from the backbone, existing pre-trained models can be retrofitted with persistent memory by installing an adapter and retraining—no architectural redesign is required. We believe that full-scale training will show dramatically stronger results; this study establishes the feasibility, the taxonomy, and the evaluation protocol that such efforts need.

Acknowledgements

The author thanks Inha University in Tashkent for research support. This work reflects the author’s ongoing inquiry into nature and human cognition.

References

- [1] Colin Raffel, Noam Shazeer, Adam Roberts, Katherine Lee, Sharan Narang, Michael Matena, Yanqi Zhou, Wei Li, and Peter J. Liu. Exploring the limits of transfer learning with a unified text-to-text transformer. *JMLR*, 21(140):1–67, 2020.
- [2] Charles Packer, Sarah Wooders, Kevin Lin, Vivian Fang, Shishir G. Patil, Ion Stoica, and Joseph E. Gonzalez. MemGPT: towards LLMs as operating systems. *arXiv preprint arXiv:2310.08560*, 2024.
- [3] Wanjun Zhong, Lianhong Guo, Qiqi Gao, He Ye, and Yanlin Wang. MemoryBank: enhancing large language models with long-term memory. In *AAAI*, 2024.
- [4] Jing Xu, Arthur Szlam, and Jason Weston. Beyond goldfish memory: Long-term open-domain conversation. In *ACL*, 2022.
- [5] Adyasha Maharana, Dong-Ho Lee, Sergey Tulyakov, Mohit Bansal, Francesco Barbieri, and Yuwei Fang. Evaluating very long-term conversational memory of LLM agents. In *Proceedings of the 62nd Annual Meeting of the ACL*, 2024.
- [6] Hong Jeong. Inhibitory cross-talk enables functional lateralization in attention-coupled latent memory. *arXiv:2603.03355 [q-bio.NC]*, 2026. <https://arxiv.org/abs/2603.03355>.
- [7] Hong Jeong. A miniature brain transformer: Thalamic gating, hippocampal lateralization, amygdaloid salience, and prefrontal working memory in attention-coupled latent memory. *arXiv:2603.07217 [q-bio.NC]*, 2026. <https://arxiv.org/abs/2603.07217>.
- [8] Endel Tulving. Episodic and semantic memory. In E. Tulving and W. Donaldson, editors, *Organization of Memory*, pages 381–403. Academic Press, 1972.
- [9] James L. McClelland, Bruce L. McNaughton, and Randall C. O’Reilly. Why there are complementary learning systems in the hippocampus and neocortex: insights from the successes and failures of connectionist models of learning and memory. *Psychological Review*, 102(3):419–457, 1995.

- [10] Dharshan Kumaran, Demis Hassabis, and James L. McClelland. What learning systems do intelligent agents need? Complementary learning systems theory updated. *Trends in Cognitive Sciences*, 20(7):512–534, 2016.
- [11] Xiang Lisa Li and Percy Liang. Prefix-tuning: Optimizing continuous prompts for generation. In *ACL-IJCNLP*, 2021.
- [12] Jean-Baptiste Alayrac, Jeff Donahue, Pauline Luc, Antoine Miech, Iain Barr, Yana Hasson, Karel Lenc, Arthur Mensch, Katie Millican, Malcolm Reynolds, Roman Ring, Eliza Rutherford, Serkan Cabi, Tengda Han, Zhitao Gong, Sina Samangooei, Marianne Monteiro, Jacob Menick, Sebastian Borgeaud, Andrew Brock, Aida Nematzadeh, Sahand Sharifzadeh, Mikolaj Binkowski, Ricardo Barreira, Oriol Vinyals, Andrew Zisserman, and Karen Simonyan. Flamingo: a visual language model for few-shot learning. In *NeurIPS*, 2022.
- [13] Yuhuai Wu, Markus N. Rabe, DeLesley Hutchins, and Christian Szegedy. Memorizing transformers. In *ICLR*, 2022.
- [14] Imanol Schlag, Kazuki Irie, and Jürgen Schmidhuber. Linear transformers are secretly fast weight programmers. In *ICML*, 2021.
- [15] Alex Graves, Greg Wayne, and Ivo Danihelka. Neural Turing machines. *arXiv preprint arXiv:1410.5401*, 2014.